Three-dimensional controlled source electromagnetic responses of an electrically conductive anomaly and a magnetically permeable anomaly

Kyubo Noh[1], Seokmin Oh[1], Soon Jee Seol[1], Ki Ha Lee[2] and Joongmoo Byun[1]
[1] Hanyang University, Department of Natural Resources and Geoenvironmental Engineering, Seoul, Korea
kyubonoh@gmail.com
osm79@hanyang.ac.kr
ssjdoolly@hanyang.ac.kr
jbyun@hanyang.ac.kr
[2] Korea Institute of Geoscience and Mineral Resources, Daejeon, Korea; formerly Lawrence Berkeley National Laboratory, California
kihalee@kigam.re.kr

SUMMARY

The controlled source electromagnetic (CSEM) responses can be affected by both conductive and permeable heterogeneities. Understanding of CSEM response due to conductive and permeable structure is very important not only for the inverse modeling of both parameters also for the design of survey parameters. We, in this research, present a three-dimensional CSEM edge-based finite element modeling algorithm which can accommodate conductive and permeable structure. The use of a direct solver secures a numerical stability even for a high magnetic permeable anomaly. The algorithm was verified against one-dimensional solution for conductive and permeable structure. With the developed algorithm, three-dimensional responses due to a conductive anomaly and a permeable anomaly were calculated and demonstrated on vector plots. The responses on each model will be analyzed using the integral equation which can give more intrinsic understanding than the differential equation.

Keywords: Conductivity, Permeability, Controlled Source Electromagnetic (CSEM) method, Forward modeling

INTRODUCTION

The controlled source electromagnetic (CSEM) method has been used to interpret subsurface anomalies with varying electrical conductivity (or its reciprocal, resistivity) in various applications such as hydrocarbon detection (Constable 2010), mineral exploration (Vallée et al. 2011), and environmental problem (Noh et al. 2014) under the conventional assumption that the magnetic permeability of subsurface is same with that of the free-space value.

However, even for some limited number of materials, higher magnetic property present in subsurface affects EM response. Thus, the EM response should be carefully interpreted when such a material distorts the CSEM response.

The consideration of a heterogeneity of magnetic permeability in EM method has been one of longstanding topics. In recent twenty years, the EM response due to three-dimensional (3D) structure of conductivity and magnetic permeability was simulated using finite difference method (Wang and Hohmann 1993; Alumbaugh et al. 1996; Chen et al. 2012), and finite element method (Mukherjee and Everett 2011). Among these, Mukherjee and Everett (2011) used edge-based finite element which represents boundary conditions naturally. However, they showed the poor convergence of the QMR solver when high magnetic permeability is included in modeling domain.

Along with these studies, EM responses due to magnetic anomalies were analyzed with physical insight and mutual coupling value (Chen et al. 2012; Mukherjee et al. 2012). However, more intrinsic understanding of physical phenomena will be more helpful to set efficient inversion strategy.

We, in this study, have developed 3D CSEM forward modeling algorithm for conductive and permeable heterogeneities using edge-based finite element method. A direct solver was used in this algorithm to secure the numerical stability. Using the developed algorithm, we will demonstrate the vector behaviors of magnetic fields due to not only a conductive anomaly also a magnetic anomaly.

DEVELOPMENT OF 3D CSEM FORWARD ALGORITHM

With ignoring displacement currents and assuming an $e^{i\omega t}$ time harmonic dependence, Maxwell equation can be re-written as below in terms of secondary field formulation.

$$\nabla \times \frac{\mu_0}{\mu} \nabla \times \mathbf{E}_S + i\omega\mu_0\sigma\mathbf{E}_S = -i\omega\mu_0\Delta\sigma\mathbf{E}_P - i\omega\mu_0\nabla \times \left(\frac{\Delta\mu}{\mu}\mathbf{H}_P\right) \quad (1)$$

Here, the electrical conductivity (σ) and magnetic permeability (μ) are variables with respect to 3D position. In this study, the primary field is accurately calculated from one-dimensional (1D) layered earth model (Pellerin et al. 1995).

The governing equation described above was solved using edge-based finite element method. We modified the CSEM modeling algorithm introduced by Chung et al. (2014) which only considers the conductivity as a spatial variable. As described in their paper, we also use direct solving method to get the solution of edge directional value of electrical secondary field. From computed electric field, magnetic field can be calculated through numerical implementation of Faraday's law.

VALIDATION OF THE ALGORITHM

We used 1D layered earth analytic solution to test the accuracy of the modified algorithm. We tested against two 1D models (1) 3 layers with the second layer of only permeable variation; and (2) 3 layers with the second layer of both conductive and permeable variations. For the 1D model (1), resistivity, relative permeability, and thickness of 3 layers are set to [100 ohm-m, 100 ohm-m, 100 ohm-m], [1.0, 2.0, 1.0], and [20 m, 10 m, semi-infinite]. In the 1D model (2), only the resistivity value of the second layer is changed into 10 ohm-m. The primary field is defined as the response of non-magnetic and 100 ohm-m half-space model.

The computed vertical magnetic components of secondary (anomalous) field due to vertical magnetic dipole of 1000 Hz at 1 m above the surface are shown in Figure 1 and 2. The receiver arrays were deployed from 5 to 150 m offset from the source at 1 m above the surface. To evaluate the numerical accuracy of 3D solution, relative error was also calculated.

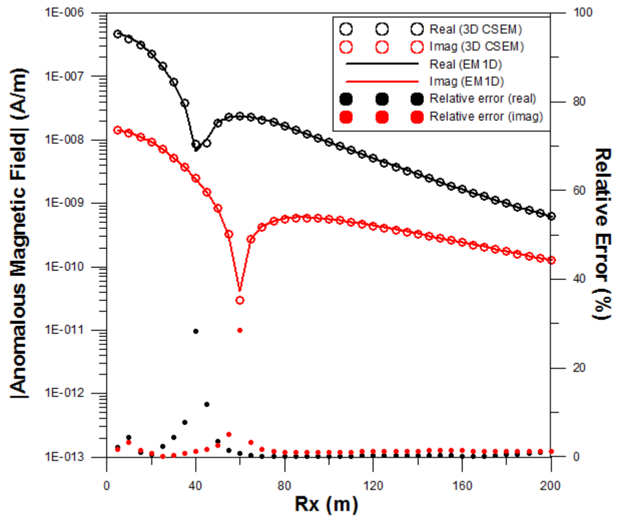

Figure 1. Comparison of 1D and 3D responses of 1D model (1) due to a 1 kHz vertical magnetic dipole.

The absolute value of magnetic field is plotted to compare the values.

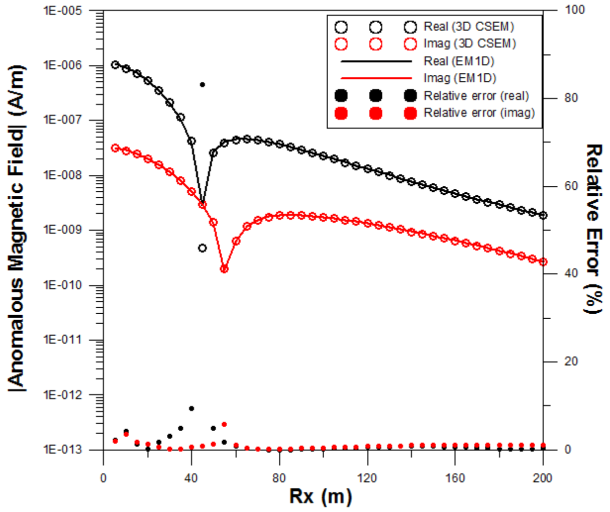

Figure 2. Comparison of 1D and 3D responses of 1D model (2) due to 1 kHz vertical magnetic dipole. The absolute value of magnetic field is plotted to compare the values.

As shown in Figure 1 and 2, most of relative error values are under 1percent except for near zero-crossing points and the mean value of all errors are around 2percent which means excellent agreement between 3D and 1D solution.

3D CSEM RESPONSES

To get the intrinsic understanding of EM responses, 3D responses of isolated anomaly models are calculated. The rectangular shaped isolated anomaly of 10 X 10 X 10 m was located at (5 m, 0 m, 25 m) as a center position in a non-magnetic and conductive half-space of 100 ohm-m. A vertical magnetic dipole source was located at (0 m, 0 m, -1 m).

We calculated anomalous fields due to two 3D models with different property of isolated body (1) 100 ohm-m of resistivity and 2.0 of relative magnetic permeability; and (2) 10 ohm-m of resistivity and 1.0 of relative magnetic permeability, i.e. (1) the permeable anomaly and (2) the conductive anomaly.

The results of secondary magnetic field for two models due to 100 Hz source are shown in Figure 3 and 4, respectively. In Figure 3, responses of real and imaginary components can be understood as a magnetic dipole response which has opposite directional behavior.

On the other hand, magnetic field caused by a conductive anomaly shown in Figure 4 shows vortex shaped propagation of magnetic field and higher intensity in imaginary component than in real component. These vector behaviors of induced magnetic field are also similar with those when the source frequency is increased to 10000 Hz (Figure 5 and 6). However, the difference in the relative intensity of real and imaginary components is reduced.

The secondary field solutions from equation (1) consists of effects from anomalies of both the conductivity and permeability. Separation of contributions from the conductivity anomaly and the permeability anomaly is not possible.

Electric and magnetic fields in the presence of both the conductivity and permeability anomalies can also be directly computed using the coupled integral equations (i.e., de Hoop 1995)

$$\mathbf{E}^S(\mathbf{r}) = \int_V \left[\mathbf{G}_J^E(\mathbf{r},\mathbf{r}')\left\{\Delta\sigma\mathbf{E}^T(\mathbf{r}')\right\} + \mathbf{G}_M^E(\mathbf{r},\mathbf{r}')\left\{i\omega\Delta\mu\mathbf{H}^T(\mathbf{r}')\right\}\right]dV \qquad (2)$$

$$\mathbf{H}^S(\mathbf{r}) = \int_V \left[\mathbf{G}_J^H(\mathbf{r},\mathbf{r}')\left\{\Delta\sigma\mathbf{E}^T(\mathbf{r}')\right\} + \mathbf{G}_M^H(\mathbf{r},\mathbf{r}')\left\{i\omega\Delta\mu\mathbf{H}^T(\mathbf{r}')\right\}\right]dV \qquad (3)$$

The right hand sides of equations (2) and (3) contain the electric/magnetic field Green's tensor and the equivalent volume source density of electric/magnetic currents defined as those within the brackets {.}, respectively. Solutions to these equations should be identical to that of equation (1). One immediate consequence is that, given the solutions **E** and **H** obtained from equation (1), equations (2) and (3) can be used to evaluate the quantitative contributions of the conductivity anomaly and the permeability anomaly on the secondary electric and magnetic fields, separately. A physical insight as to the effect of the conductivity anomaly and the permeability anomaly can therefore be realized.

CONCLUSION

This study was started to understand underlying physics of CSEM response due to conductive and permeable structures. Thus, in this study, we have developed 3D edge-based finite element CSEM modeling algorithm which successfully deals with conductive and permeable heterogeneities. The finite element solution was compared against 1D solution and the result showed good agreement. By the use of the developed forward modeling algorithm, scattered electromagnetic responses due to a conductive anomaly and a permeable anomaly were calculated. The EM responses from these two models showed very different behaviors. In following studies, systematic analysis on secondary electric/magnetic field will be conducted by using integral representation of scattered electromagnetic wave.

ACKNOWLEDGEMENTS

This work was supported by the Human resources Development program (*No.* 20134010200520) of the Korea Institute of Energy Technology Evaluation and Planning (KETEP) grant funded by the Korea government Ministry of Trade, Industry and Energy. One of the author, Kyubo Noh was supported by NRF (National Research Foundation of Korea) grant funded by Korea government (NRF-2012H1A2A1009568-Global Ph. D. Fellowship Program). Work by Ki Ha Lee was partially supported by the Basic Research Project of the Korea Institute of Geoscience and Mineral Resources funded by the Ministry of Science, ICT and Future Planning, Republic of Korea.

REFERENCES

Alumbaugh, D. L., Newman, G. A., Prevost, L., and Shadid, J. N. (1996) Three-dimensional wideband electromagnetic modeling on massively parallel computers. Radio Science 31:1-23

Chen, J., Tompkins, M., Zhang, P., Wilt, M., and Mackie, R. (2012) Frequency-domain EM modeling of 3D anisotropic magnetic permeability and analytical analysis. SEG Technical Program Expanded Abstracts 1-5. doi: 10.1190/segam2012-0308.1

Chung, Y., Jeong-Sul, S., Tae Jong, L., Hee Joon, K. & Changsoo, S. (2014) Three-dimensional modelling of controlled-source electromagnetic surveys using an edge finite-element method with a direct solver. Geophysical Prospecting in press

Constable, S`. (2010) Ten years of marine CSEM for hydrocarbon exploration. Geophysics 75:75A67-75A81

de Hoop AT (1995) Handbook of radiation and scattering of waves, Academic Press, London

Mukherjee, S., and Everett, M. (2011) 3D controlled-source electromagnetic edge-based finite element modeling of conductive and permeable heterogeneities. Geophysics 76:F215-F226

Mukherjee, S., Everett, M. E., Benavides, A. I., and Fernandes, R. (2012) Mutual coupling of conductive, permeable targets and its effects on CSEM response. SEG Technical Program Expanded Abstracts 1-6. doi: 10.1190/segam2012-1505.1

Noh, K., Chung, Y., Seol, S. J., Byun, J., and Uchida, T. (2014) Three-dimensional inversion of CSEM data: Water leak detection using a small-loop EM method. Journal of Applied Geophysics 102:134-144

Pellerin, L., Labson, V. F., and Pfeifer, M. C. (1995) VETEM-A very early time electromagnetic system. Symposium on the Application of Geophysics to Engineering and Environmental Problems (SAGEEP) Proceedings 725-731

Vallée, M., Smith, R., and Keating, P. (2011) Metalliferous mining geophysics - State of the art after a decade in the new millennium. Geophysics 76:W31-W50

Wang, T., and Hohmann, G. (1993) A finite-difference, time-domain solution for three-dimensional electromagnetic modeling. Geophysics 58:797-809

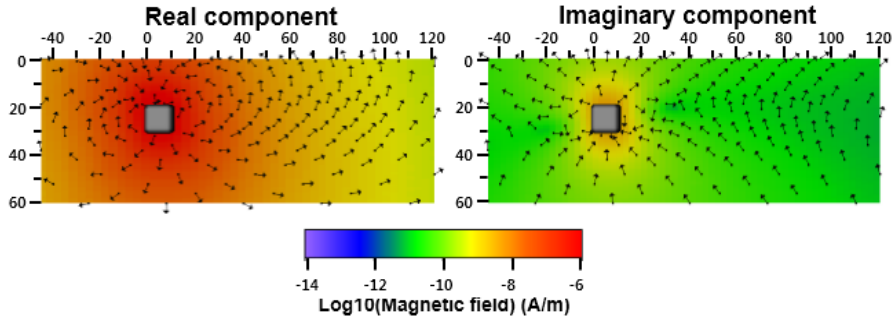

Figure 3. The cross-section (y = 0 m) of computed secondary magnetic field due to magnetically permeable anomaly in 100 ohm-m half space. A 100 Hz vertical magnetic dipole source is employed.

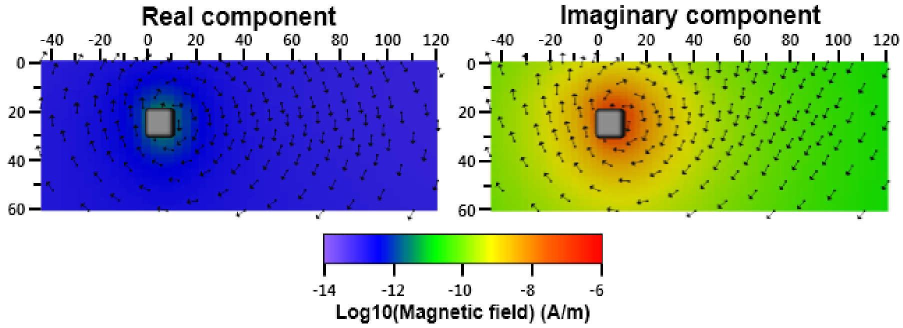

Figure 4. The cross-section (y = 0 m) of computed secondary magnetic field due to conductive anomaly in 100 ohm-m half space. A 100 Hz vertical magnetic dipole source is employed.

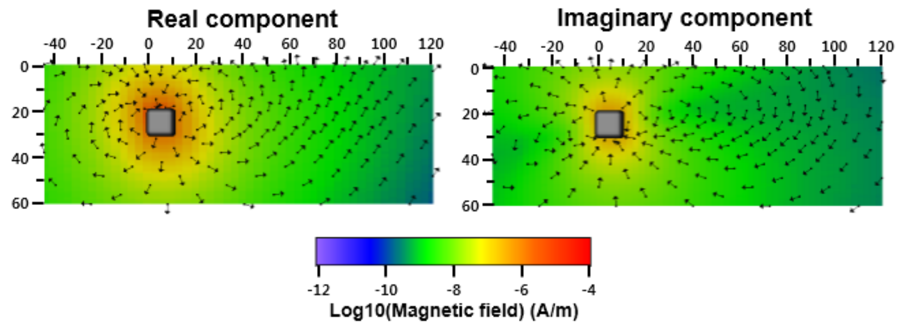

Figure 5. The cross-section (y = 0 m) of computed secondary magnetic field due to magnetically permeable anomaly in 100 ohm-m half space. A 10000 Hz vertical magnetic dipole source is employed.

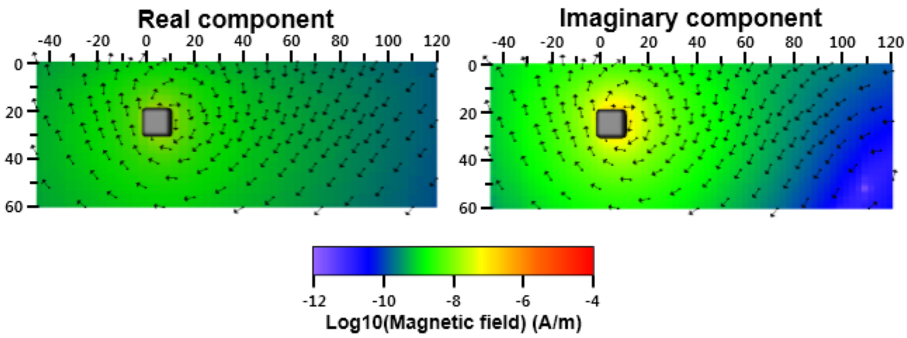

Figure 6. The cross-section (y = 0 m) of computed secondary magnetic field due to conductive anomaly in 100 ohm-m half space. A 10000 Hz vertical magnetic dipole source is employed.

.